12th Ablation Workshop

Lexington, KY
November 9th, 2022

Coupling CFD and Material Response for Analysis of Mars Entry

John M. Thornton[1], Dinesh K. Prabhu[1], Jeremie B.E. Meurisse[1],
Arnaud P. Borner[1], Joshua D. Monk[2], Brett A. Cruden[1]
Analytical Mechanics Associates, Inc. at NASA Ames Research Center[1], NASA Ames Research Center[2]

Objective

The objective of this work is to showcase and analyze the coupling between the material response and the aerothermal environment in simulating the Mars atmospheric entry of the Mars Science Laboratory (MSL) on an axisymmetric sphere case. In preparation for Mars 2020 post-flight analysis, the predictive material response capability is benchmarked against flight data from MSL. This work represents an important milestone toward the development of validated predictive capabilities for designing thermal protection systems for planetary probes. Future work will include utilizing this coupling in full 3D simulations of both MSL and Mars 2020.

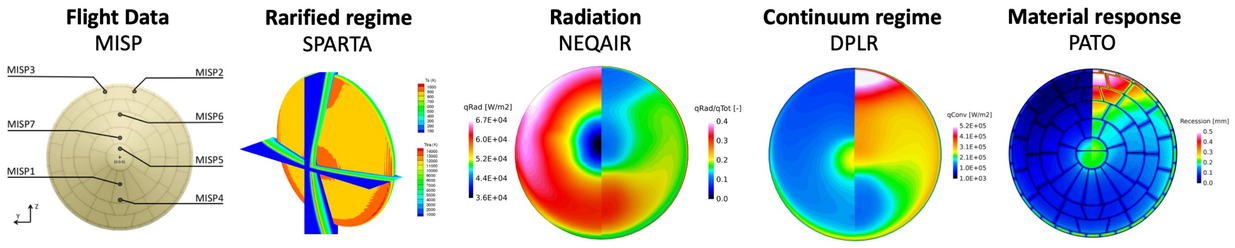

Fig. 1 Diagram showing the location of the MISP plugs on the MSL heatshield and highlighting the codes used in this study. The MISP plugs contained thermocouples at varying depths to provide in-depth temperature data during the MSL entry.

Coupling Process

As shown in Figure 2, the workflow is divided into the following steps:

1. The aerothermal properties are computed in the Data Parallel Line Relaxation (DPLR) code [1] and used with the Nonequilibrium air radiation (NEQAIR) program [2] to compute radiative heating.
2. The thermal response inside the material is computed with the Porous material Analysis Toolbox based on Open-FOAM (PATO) [3,4,5] using a fixed blowing correction parameter λ.
3. The pyrolysis gases computed with PATO are used as inputs to a blowing boundary condition within DPLR.
4. The new environment properties from DPLR are used in NEQAIR to provide an updated solution
5. Both the updated aerothermal environment and radiative heating are used in PATO with no blowing correction in a heat flux boundary condition.
6. Steps 3-5 are then repeated until convergence in surface temperature is obtained.

Convergence in the radiative heating is generally achieved before surface temperature, at which point the radiative heating is no longer updated. Char mass loss rates are forced to zero to produce a non-receding surface condition.

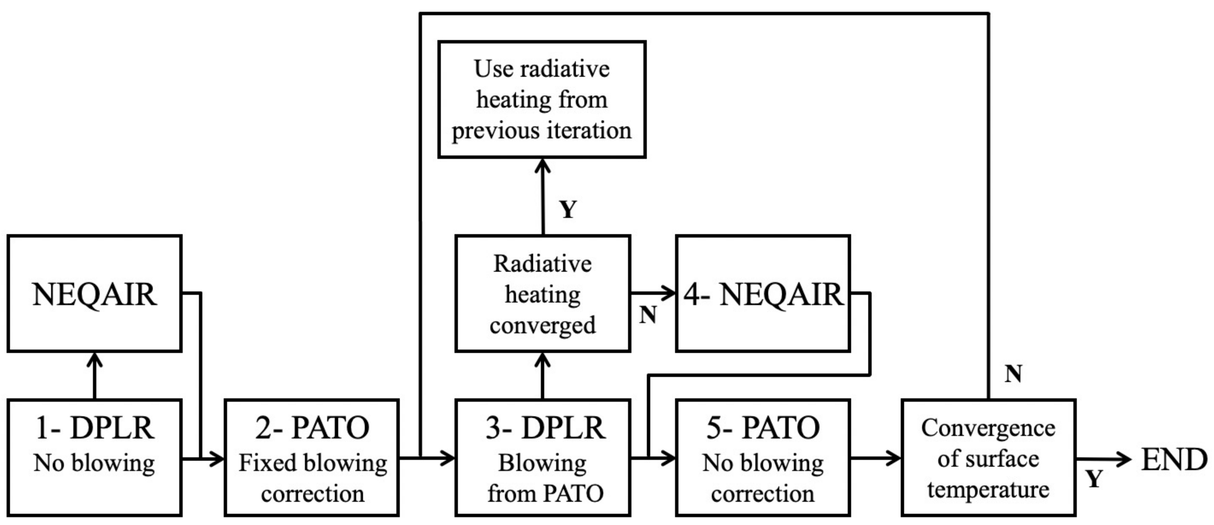

Fig. 2 Diagram showing the coupling process. DPLR and NEQAIR provide inputs to PATO which is initially run with a fixed blowing correction parameter λ. The blowing rates and species computed by PATO are then used as inputs to DPLR in a blowing boundary condition. Aerothermal environment (DPLR), radiative heating (NEQAIR), and material response (PATO) computations are then iterated without blowing corrections.

Coupling Tool

- The coupling tool is a python code created to interface the different simulation tools (PATO, DPLR, and NEQAIR) used in the coupled simulations.
- Currently tested with a 2D sphere case using MSL entry conditions at MISP1.
- Includes an option for running with or without radiation from NEQAIR and supports either B' or heat flux based boundary conditions.

Aerothermal Environment

- Chemical and thermal nonequilibrium
- 20 species model for Mars atmosphere in consideration of pyrolysis gases blown from material
- 12 lines of sight used with NEQAIR for radiative heating computations in sphere case

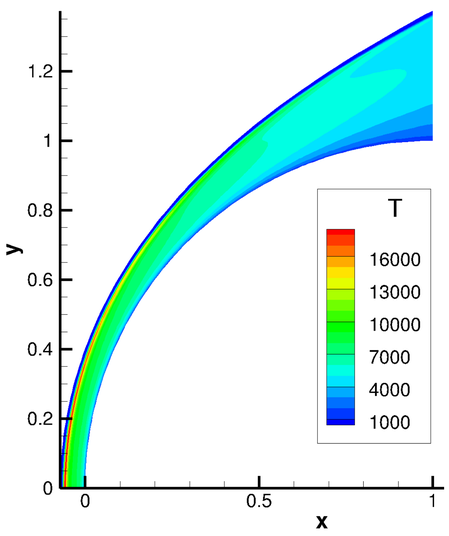

Fig. 3 Sphere case

Material Response

The material response model in PATO is a mass and heat transfer model for porous reactive materials containing several solid phases and a single gas phase [4]. The following assumptions are made:

- Local thermal equilibrium at the pore scale
- A heat flux boundary condition at the surface
- Equilibrium chemistry

Blowing Correction

The material response requires the pressure (p_w) and heat transfer coefficient (C_H) at the heatshield surface along with the enthalpy at the boundary layer edge (h_e) which are given by DPLR. The blowing correction for the initial iteration is applied in the following way:

$$C'_H = C_H \frac{\ln\{1 + 2\lambda(B'_{\text{pyro}} + B'_{\text{char}})\}}{2\lambda(B'_{\text{pyro}} + B'_{\text{char}})}$$

C'_H	modified heat transfer coefficient
λ	blowing correction parameter
B'_{pyro}	nondimensional pyrolysis gas blowing rate
B'_{char}	nondimensional char blowing rate (zero in this study)

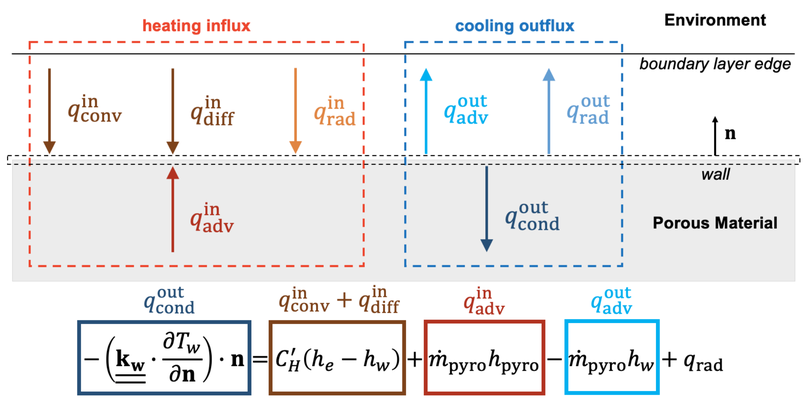

Fig. 4 Surface energy balance

Results for Axisymmetric Sphere Case

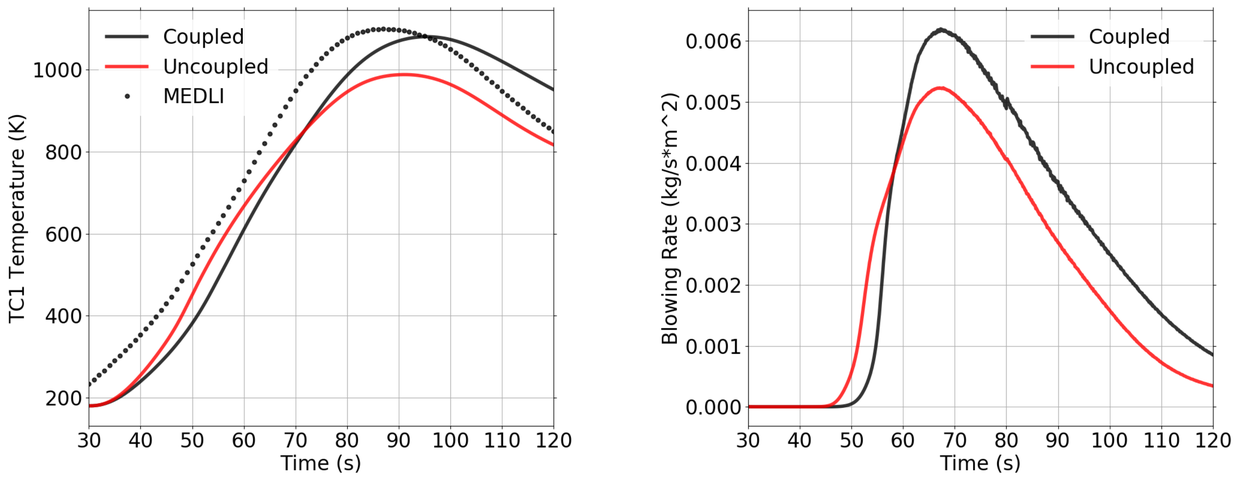

Fig. 5 Temperature at TC1 depth (left) and blowing rate (right) profiles at the stagnation point for the coupled and uncoupled sphere case. The temperature plot includes the TC1 flight data from MEDLI for comparison.

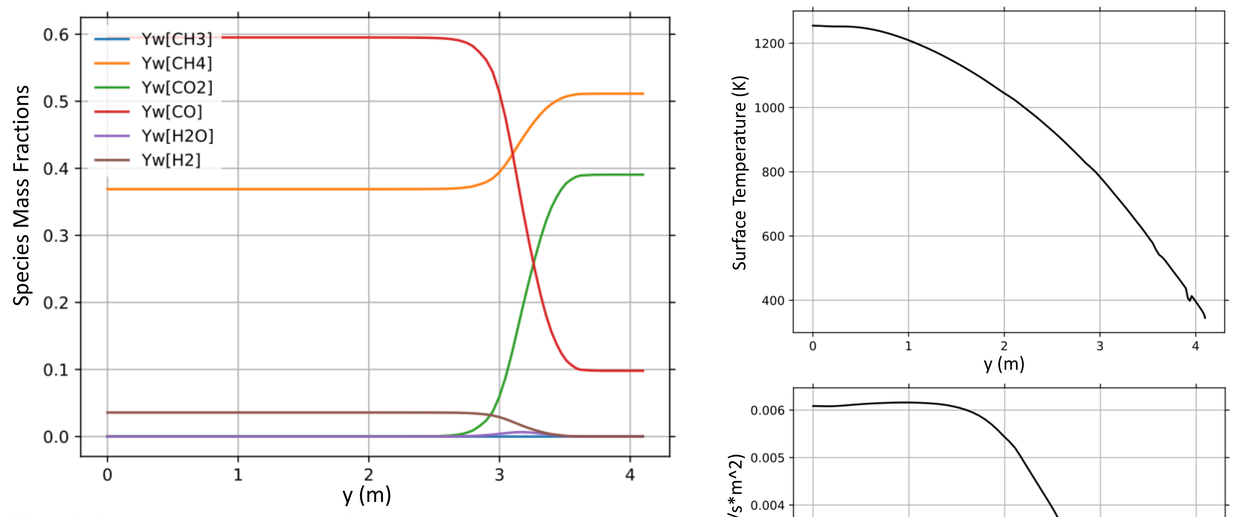

Fig. 6 Species mass fractions (top), temperature (top right), and blowing rate (right) at the surface for the sphere case at peak heating.

References

[1] M.J. Wright et al. (2009), DPLR Code User Manual: Acadia-Version 4.01.1.
[2] E. Whiting et al. (1996) NASA RP-1389.
[3] J. Lachaud et al. (2014), J Thermophys Heat Tran, 28, 191–202.
[4] J. Lachaud et al. (2017), Int J Heat Mass Tran, 108, 1406–1417.
[5] J. B.E. Meurisse et al. (2018), Aerosp Sci Tech-nol, 76, 497-511.